Geomechanics and Engineering, Vol. 3, No. 4 (2011) 323-337
DOI: http://dx.doi.org/10.12989/gae.2011.3.4.323

Characterizing the geotechnical properties of natural, Israeli, partially cemented sands

Sam Frydman*

Faculty of Civil & Environmental Engineering, Technion – Israel Institute of Technology, Haifa, Israel

(Received April 14, 2011, Revised September 20, 2011, Accepted September 20, 2011)

Abstract. Israel's coastal region consists, mainly, of Pleistocene and Holocene sands with varying degrees of calcareous cementation, known locally as "kurkar". Previous studies of these materials emphasized the difficulty in their geotechnical characterization, due to their extreme variability. Consequently, it is difficult to estimate construction stability, displacements and deformations on, or within these soils. It is suggested that SPT and Menard pressuremeter tests may be used to characterize the properties of these materials. Values of elastic modulus obtained from pressuremeter tests may be used for displacement analyses at different strain levels, while accounting for the geometric dimensions (length/diameter ratio) of the test probe. A relationship was obtained between pressuremeter modulus and SPT blow count, consistent with published data for footing settlements on granular soils. Cohesion values, for a known friction angle, are estimated, by comparing field pressuremeter curves to curves from numerical (finite element or finite difference) analyses. The material analyzed in the paper is shown to be strain-softening, with the initial cohesion degrading to zero on development of plastic shear strains.

Keywords: pressuremeter; cemented sand; standard penetration test; modulus of elasticity; cohesion; strain softening; numerical analysis.

1. Introduction

The quaternary formations of Israel's coastal region developed during a series of interchanging ingressions and regressions of the Mediterranean Sea, accompanied by sedimentation cycles of marine and continental deposits. The greater part of the formations consists of Pleistocene and Holocene layers of sands with varying degrees of calcareous cementation, known locally as "kurkar. The mineralogy and petrography of these materials has been extensively studied (e.g. Gavish and Friedman 1969, Bakler *et al.* 1972). The sand fraction originates in the Nile and is transported by the East Mediterranean longshore currents, and then deposited by water and wind. The sand is made up mainly of light minerals – predominantly quartz, with a few grains of feldspar. Heavy minerals amount to 0.1%-5%, and include hornblende, augite, zircon, rutile and some minor species. The quartz grains are sub-angular to sub-rounded, uniformly graded with a mean size of about 0.2 mm. The cementation is by calcite, and is a result of the dissolution of skeleton debries and precipitation in place, together with addition of calcium carbonate from fluviatile or meteoric solutions percolating

*Professor, E-mail: cvrsfsf@technion.ac.il

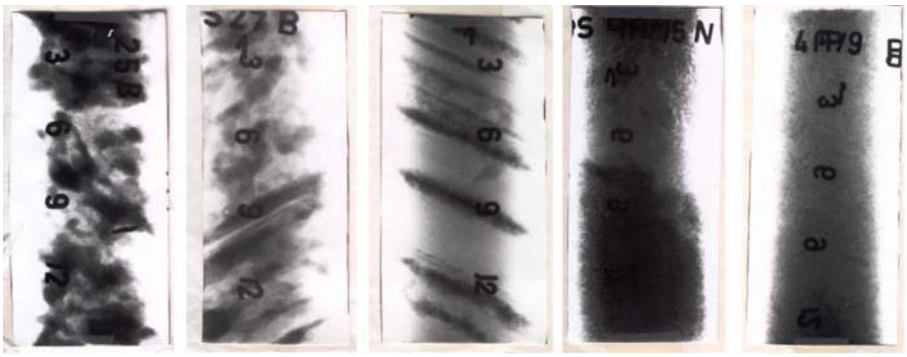

(a) (b) (c) (d) (e)

Fig. 1 X-ray photographs of undisturbed kurkar-sand samples (sample height 150 mm) (after Frydman *et al.* 1980)

through the interparticle pore space. Carbonate content varies typically from 20%-50%.

Previous geotechnical studies of these materials have been reported by Frydman (1979), Frydman *et al*. (1979), Wiseman *et al.* (1981), Frydman *et al.* (1980), Frydman (1982), and Frydman (1987). All of these studies emphasized the difficulty in geotechnical characterization of kurkar deposits, due to their extreme variability. This paper presents an approach for this geotechnical characterization which has developed over a number of years of dealing with kurkar in a variety of engineering problems.

The kurkar deposits observed along the Israeli Mediterranean coast take various forms: sandstone plates of various thicknesses and orientations separated by clean dune sand, strongly cemented concretions floating in a sand matrix, and variably cemented sand. Fig. 1 shows x-ray photographs of cylindrical specimens cored from frozen block samples (Frydman *et al.* 1980). The extreme

(a) (b)

Fig. 2 Kurkar profiles in Tel-Aviv: (a) weakly cemented and (b) strongly cemented

variability in internal structures encountered over short distances, seen in Fig. 1, illustrates the basic difficulty in characterizing the global, operative, geotechnical parameters of the kurkar. Fig. 1(a) shows a sand matrix with randomly floating strong, cemented concretions; in Fig. 1(b), the top of the specimen is a sand matrix with floating cemented concretions, while the bottom portion contains sand and inclined cemented plates; Fig. 1(c) shows a specimen made up completely of inclined layers of sand and cemented plates; Fig. 1(d) shows weakly cemented sand in the upper portion and dense, strongly cemented sand in the lower portion; and Fig. 1(e) shows a specimen consisting of clean, noncemented sand varying in density from loose at the top to dense at the bottom. Examples of some kurkar outcrops are shown in Fig. 2, a weakly cemented material shown in Fig. 2(a), and a strongly cemented one in Fig. 2(b).

2. Lessons learnt from coastal-cliff instabilities

The central part of the Mediterranean coastline, between Tel-Aviv and Netanya, is bordered by a linear escarpment, up to 50 m high, composed mainly of kurkar deposits. As a result of recurring, shallow slips along this cliff (e.g. Fig. 3), an investigation of its stability was carried out and reported by Wiseman *et al.* (1981), as summarized briefly in the following. A schematic, typical cross-section of the escarpment is shown in Fig. 4. The thickness of unit 2 may be up to 24 m, of unit 3 up to 38 m, of unit 4 up to 6 m, and of unit 5 up to 8 m. Kurkar units 2 and 3 usually constitute the major portion of the cliff profile, and consequently they largely control slope stability. Triaxial tests, under saturated conditions, were performed on a limited number of specimens cored from frozen block samples taken from these two units at confining pressures of between 25-150 kPa, indicating a friction angle, ϕ', of 35°-37°, regardless of cementation, and a cohesion value, c', dependent on the degree of cementation. Unit 3 is weakly cemented, and may be conservatively

Fig. 3 A shallow slip in a kurkar cliff

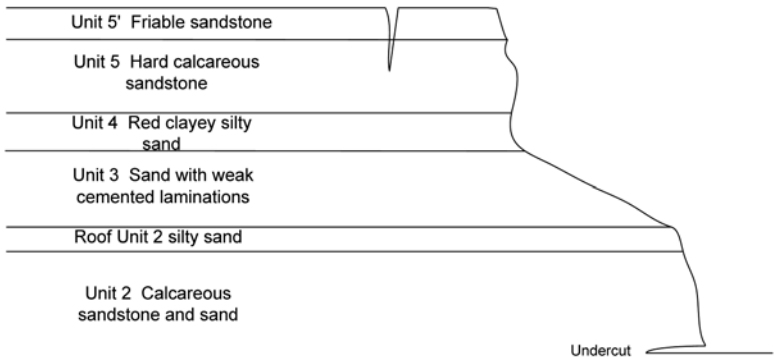

Fig. 4 A typical schematic cross-section of kurkar escarpments

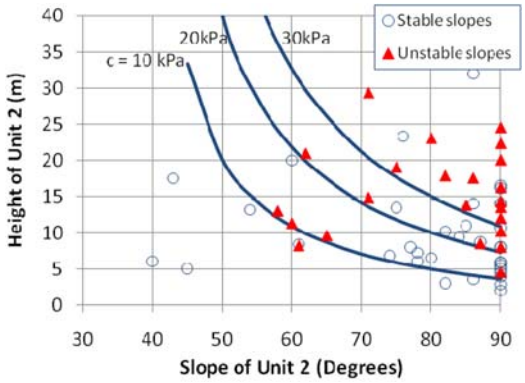

Fig. 5 Stability chart for kurkar escarpments near Tel-Aviv

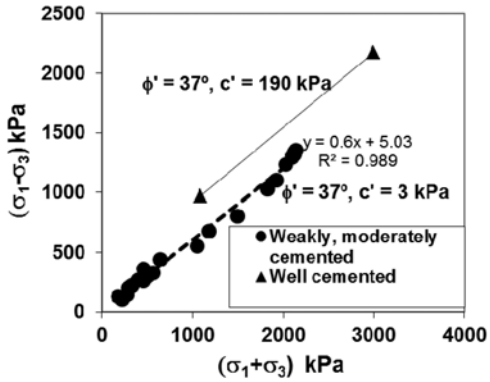

Fig. 6 Triaxial failure stresses from tests on undisturbed kurkar samples

considered as sand, with zero cohesion and a friction angle of 35°-37°. On the other hand, the cementation present in unit 2 provides it with a certain amount of cohesion. The estimation of a reasonable, global design value for this cohesion represents a major engineering challenge in dealing with this material. In view of the large variability observed in the degree of cementation within the material, field observations were used for estimation of this parameter. A geodetic survey was carried out of eighty three cliff section slopes and heights along the cliff face, noting evidence of their stability or instability. Fig. 5 shows data for slopes in which unit 2 dominated, indicating slope inclination versus height, and differentiating between stable and unstable slopes. Superimposed on this figure are curves obtained from Taylor's stability chart (Taylor 1937), showing the stable height of a homogeneous soil slope as a function of slope inclination for a soil with a unit weight, γ, of 20 kN/m^3, $\phi' = 35$, and c' varying between 10 kPa to 30 kPa. A cohesion value of about 10 kPa appears to provide a reasonable lower bound to the points representing instability within slopes consisting predominantly of unit 2. A further opportunity for estimating global strength parameters arose as a result of the observation of a well defined slide which occurred during the investigation in a predominantly unit 2 slope. Slope stability analysis indicated that both the occurrence of the slide and the shape and location of the slip surface were consistent with strength parameters $c' = 20$ kPa and $\phi' = 35$.

3. Testing of undisturbed samples

The feasibility investigation of a southern coastal site for a nuclear power plant (Frydman *et al.* 1980) provided the opportunity for carrying out triaxial tests on undisturbed samples of kurkar. The test specimens were prepared from block samples extracted from the site, both from the soil surface and from excavated pits, and then frozen and cored in the laboratory. Additional sampling and testing was performed more recently on samples taken from sites in Tel-Aviv for design of the planned Tel-Aviv Metro lines. Fig. 6 shows strength results from these tests, indicating that weakly and moderately cemented kurkar could be considered to share a common strength envelope with strength parameters $c' = 3$ kPa and $\phi' = 37$. This friction angle was found to be consistent with results of a test performed on well cemented kurkar as shown in the figure, but in this case a

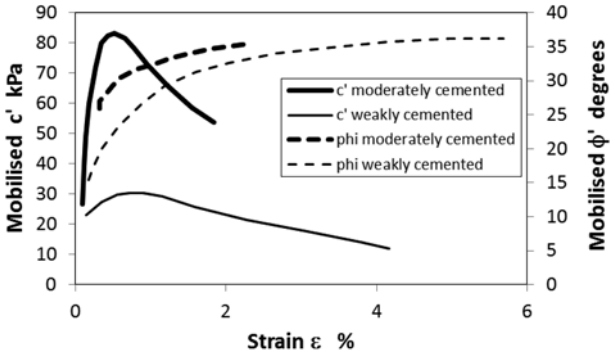

Fig. 7 Development of c' and ϕ' with strain in triaxial tests

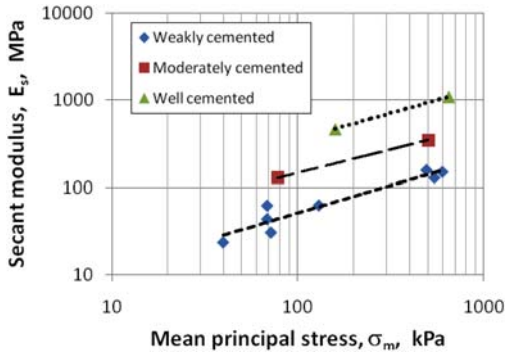

Fig. 8 Secant modulus, E_s, at 1/3 of failure stress, versus mean normal stress

significant cohesion of 190 kPa was observed. Fig. 7 shows the mobilisation of cohesion and friction angle with strain, indicating that cohesion reaches a maximum value at a fairly small strain, and then decreases, presumably due to breakdown of cementation. On the other hand, the friction angle increases up to failure. This breakdown in cohesion may explain the convergence of strength results from weakly and moderately cemented kurkar soils, since the moderate cementation is presumably largely lost by the time failure is reached. In contrast, Fig. 8 shows secant modulus, E_s, as a function of mean normal stress, σ_m, at one-third of the failure stress. Here, where the material is still far from failure, a significant difference is observed between the weakly cemented and the moderately cemented materials.

The above discussion indicates that while the friction angle of the kurkar deposits can be reasonably taken as 35°-37°, estimation of representative cohesion and modulus values is much more difficult, presumably depending on the degree of cementation. For example, c' values between 3-190 kPa were indicated above, on the basis of various tests and analyses. In view of the variability in cementation over small distances, it appears that choice of global parameters would best be based on back estimation from field observations or from field tests performed on significant soil volumes. The back calculations performed on the basis of observations of slope cliff stabilities are a good example of this approach; back calculations from in-situ loading tests to failure could provide an alternative approach. This latter option is developed in the following sections of the paper.

4. Use of the Menard pressuremeter

As stated above, back calculation from results of loading tests could offer a reasonable approach for the estimation of in-situ global parameters of kurkar. The pressuremeter provides a method of carrying out lateral loading tests within boreholes. Ideally, it would be desirable to use a self-boring pressuremeter (e.g. Hughes *et al.* 1977), but this would not generally penetrate the kurkar profiles. Consequently, a Menard pressuremeter (Komornik *et al.* 1969, Baguelin *et al.* 1978), in which tests are carried out in a pre-drilled borehole, may be employed. A schematic layout of the Menard pressuremeter is shown in Fig. 9. During performance of a pressuremeter test, pressure in the probe is increased, transferring lateral stress to the surrounding soil. Deformation of the probe, and

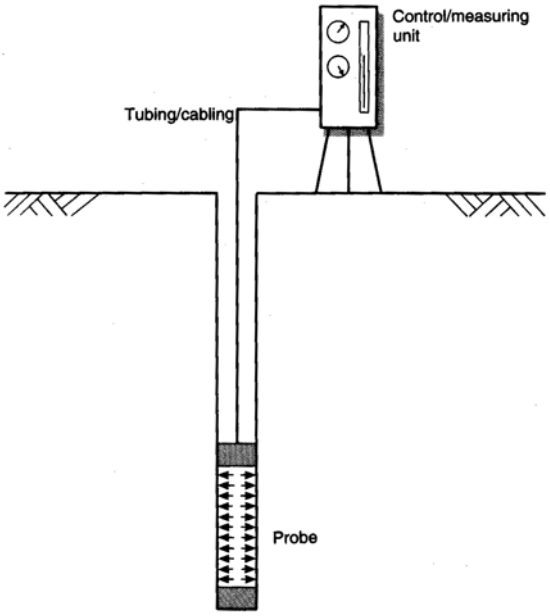

Fig. 9 Schematic layout of the Menard pressuremeter (after Clayton *et al.* 1995)

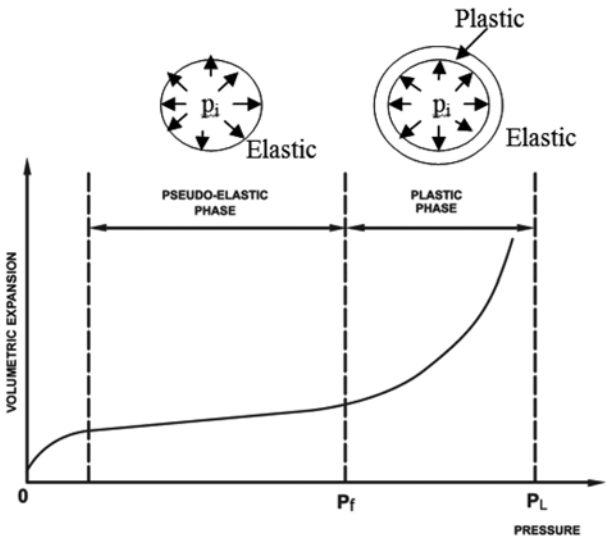

Fig. 10 Typical pressuremeter volume change versus pressure curve

resultant displacements in the surrounding soil, are assumed to be only radial, resulting in an axi-symmetric, plane strain loading condition. Volume change of the probe, related directly to radial displacement of the probe-soil contact, is measured in the measuring unit on the soil surface. Fig. 10 shows a schematic volume-change versus pressure curve representing a typical result of a pressuremeter test. This curve may be interpreted assuming a linear elastic, perfectly plastic model for the soil behavior. Three zones are indicated - the first is the range of pressure in which good contact is established between the probe and the soil. In the second, linear zone, the soil behaves pseudo-elastically, and in the third zone, following a pressure p_f, a plastic annulus develops and expands around the probe-soil contact until failure occurs at the limit pressure, p_L. The pseudo-elastic and plastic portions of the pressuremeter curve each enable estimation of particular geotechnical parameters, as discussed below.

4.1 The pseudo-elastic range

Assuming linear elastic behavior in this range, and axi-symmetric, plane strain conditions, the straight portion of the curve allows estimation of the pressuremeter elastic modulus, *Ep*, from the equation (Gibson and Anderson 1961)

$$Ep = (1 + \nu).\, 2V.\, \Delta p/\Delta V \tag{1}$$

where ν = Poisson's ratio, V = probe volume and $\Delta p/\Delta V$ = inverse gradient of the linear portion of the curve.

It has been suggested (e.g. Mair and Muir Wood 1987) that a value of elastic modulus more consistent with field behavior is obtained by using the gradient of an unload-reload cycle in Eq. (1),

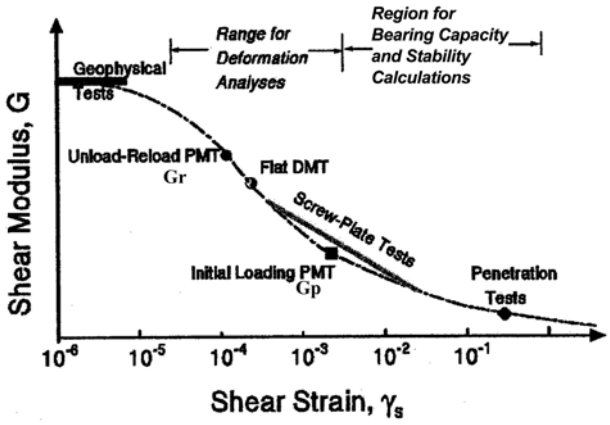

Fig. 11 Dependence of soil rigidity on shear strain level (FHWA 2002)

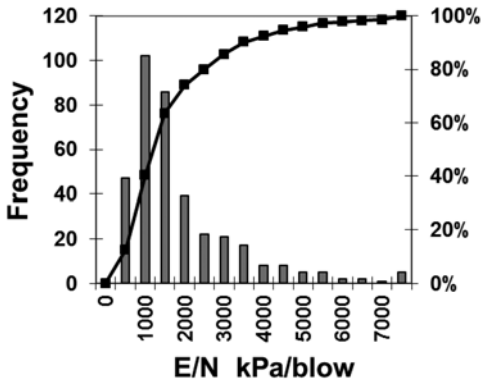

Fig. 12 Histogram of ratio between pressuremeter modulus/SPT blow count, *Ep*/*N*

this value being defined as *Er*. In fact, it is likely that in view of the non-linear, strain dependence of *E*, the values *Ep* and *Er* (or corresponding shear modulus values, *Gp* and *Gr*) correspond to different strain levels, as suggested in Fig. 11 (FHWA 2002).

A number of Menard pressuremeter tests were carried out in kurkar profiles as part of the investigation for the Tel-Aviv Metro project. The pressuremeter probe length is 360 mm, and its diameter is 64 mm. It is confined at top and bottom by guard cells of the same diameter, and lengths 180 mm, in which the pressure during test is kept slightly below that in the probe. The guard cells are intended to ensure plane, radial strain conditions in the soil adjacent to the probe during the test. The results of these tests may be used, directly, to estimate elastic modulus values. However, these tests are expensive, and not always simple to perform in the kurkar profiles. The borehole needs to be kept open until the pressuremeter is inserted and the test is performed, and probes sometimes become stuck at depth. Furthermore, the probe membranes are often torn by jagged kurkar on the borehole surface. Consequently, it was decided to investigate whether there is a relationship between elastic modulus obtained from pressuremeter tests, and results of adjacent standard penetration tests (SPT), which are commonly performed during drilling operations in granular profiles in Israel. The SPT's are generally performed using a donut hammer, with a trigger release for free-fall. As many of the early pressuremeter tests in the Metro investigation were performed without unload-reload cycles, the relationship between *Ep* and SPT blow count, *N*, was first considered. SPT's were performed immediately above and below each pressuremeter test, and the average of the two *N* values was used in preparation of Fig. 12, which shows a histogram of *Ep*/*N*. The *Ep* values correspond to cavity strains of the order of 0.005-0.01. The 50% value and median of *Ep*/*N*, were found to be approximately 1,200 kPa/blow. Fig. 13 shows the relationship between *Er* and *Ep* from tests in which unload-reload cycles were done, showing that $Er \approx 2Ep$.

On the basis of these results, the average, in-situ modulus of kurkar soils may be related to SPT blow count, *N*, through the relationships

$$\text{Small strain (}\sim 0.01\%\text{); } E \text{ (kPa)} \approx 2{,}400\ N \tag{2a}$$

$$\text{Medium strain (}\sim 0.2\%\text{); } E \text{ (kPa)} \approx 1{,}200\ N \tag{2b}$$

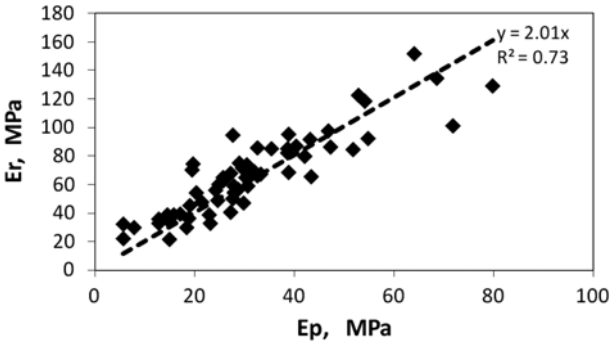

Fig. 13 Relationship between *Ep* and *Er*

Other relationships between E and N in granular soils have been reported in the literature

Stroud (1988) suggested $E = 1{,}750\ N$ kPa/blow (3)

Schmertmann (1970) suggested $E = 2q_c$, where q_c is the cone penetration tip resistance. Adopting the relationship $q_c/N = 450$ kPa/blow (Weiher and Davis 2004), Schmertmann's relationship becomes

$$E\ (\text{kPa}) = 900\ N \tag{4}$$

Lunne and Christoffersen (1985) suggested

$$E\ (1-\nu)\ /\ [(1+\nu)(1-2\nu)] = 4q_c - 5q_c$$

For Poisson's ratio, $\nu \sim 0.25$, and adopting the above relation between q_c and N, this becomes

$$1{,}500\ N \le E\ (\text{kPa}) \le 1{,}875\ N \tag{5}$$

Weiher and Davis (2004), back-calculated shear modulus, G, from published, measured settlements of deep and shallow foundations, and related the resulting modulus to SPT N values through the relationship $G/N = 1{,}300(1-\nu)$ kPa/blow. Taking $\nu = 0.25$, and recognizing that $E = 2G(1+\nu)$, the following relationship is obtained between E and N

$$E\ (\text{kPa}) \approx 2{,}440\ N \tag{6}$$

According to Bowles (1996), Japanese design standards suggest

$$E\ (\text{kPa}) = (2{,}600 \text{ to } 2{,}900)\ N \tag{7}$$

Overall, the orders of magnitude of all of these relations, except that of Schmertmann (1970), are consistent with Eqs. (2), despite their reference to uncemented rather than cemented granular soils.

In order to further study this relationship, the author has reanalyzed foundation settlement data presented for uncemented granular soils by Burland and Burbidge (1985). In their original analyses, Burland and Burbidge related measured settlements to SPT blow counts, and included measurements obtained from penetrometer tests, translating them to SPT blow counts using available correlations, and also from oedometer test results. Weiher and Davis (2004) also used this data, including the penetrometer results, in developing their relationship between G and N. In the present analysis, only the SPT data have been considered. Furthermore, in order to minimize effects of foundation shape, only settlements of foundations with length to breadth ratios (L/B) of 2 or less, representing the

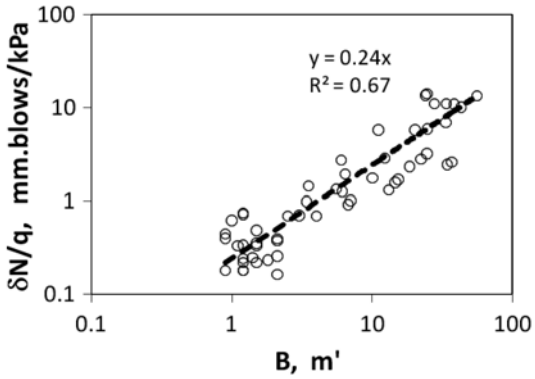

Fig. 14 Settlement data of Burland and Burbidge (1985): foundations with $L/B \leq 2$

majority of cases studied, have been considered. Fig. 14 shows $\delta N/q$ versus B for these cases, where δ is foundation settlement in mm, q is foundation contact pressure in kPa, and B is foundation width in m. A reasonable, straight line relationship is noted, expressed by

$$\delta N/q = 0.24B \tag{8}$$

The standard deviation of the slope of the line is 0.15.

For an elastic soil, the settlement of a surface footing is given by (e.g. Giroud 1968)

$$\delta = \{qB(1-\nu^2)/E\}.I \tag{9}$$

where I is a shape factor, and for $L/B \leq 2$, an average value may be taken as $I \approx 1.1$. Poisson's ratio, ν, is assumed to be equal to 0.25. Rearranging Eq. (9), and using units consistent with those used in Eq. (8), and E in kPa, the following expression is obtained

$$\delta E/q \approx 1030B \tag{10}$$

Comparing Eqs. (8) and (10), the following relationship is obtained between E and N, based on the average line in Fig. 14 from Burland and Burbidge's data for settlements of foundations with $L/B \leq 2$

$$E \approx (1030N)/0.24 \approx 4{,}300N \tag{11}$$

In order to compare Eqs. (2) and (11), it must be realized that the values of Er and Ep appearing in Eqs. (2) were based on analysis of Menard pressuremeter tests (using Eq. (1)), in which $L/B \approx 11$ (including the lengths of the guard cells). Eq. (1) takes no account of the influence of L/B on displacements, but is based on the assumption of plane strain, which is equivalent to assuming that the pressuremeter probe is infinitely long. It is reasonable to assume that a shorter ($L/B < 2$) pressuremeter probe would develop a significantly smaller horizontal displacement, so resulting in a higher estimated elastic modulus. If a shape factor relevant to pressuremeter loading is considered, and is assumed similar to the factor I in Eq. (9) for foundation loading, its value, for $L/B = 11$, would be $I \approx 2.0$ (rather than approximately 1.1, as it is for $L/B \leq 2$). It would, therefore, appear reasonable that the displacements measured in the pressuremeter tests were of the order of 2/1.1 = 1.8 times those expected if L/B of the pressuremeter probe was ≤ 2. Consequently, comparison between Eqs. (2) and (11) requires that the coefficient in Eq. (2) be multiplied by 1.8, resulting in

Small strain: E (for $L/B \leq 2$) $\approx 4300N$ (12a)

Medium strain: E (for $L/B \leq 2$) $\approx 2400N$ (12b)

Eq. (12a) compares well with Eq. (11). This suggests that Er values, obtained from unload-reload curves of Menard pressuremeter tests may be used as in-situ E values for estimation of foundation settlements at common working loads (as suggested by Mair and Muir Wood 1987), but they must be adjusted for different foundation L/B ratios. It also appears that SPT blow counts can be used for estimation of E values, through Eq. (2) developed here, or through Eq. (11) based on Burland and Burbidge; in either case account must be taken of the L/B ratio of the foundations.

4.2 The plastic range

Several solutions have been published for undrained cohesion of a frictionless soil, using the plastic portion of the pressuremeter curve (e.g. Gibson and Anderson 1961, Palmer 1972, Menard 1975). Hughes *et al.* (1977) developed an approach for evaluating the friction angle, ϕ' and dilation angle, ψ, of a cohesionless soil. Kurkar may be considered as a cohesive-frictional material, with a friction angle, as obtained from triaxial tests, of about 37°. The purpose of the present investigation was to try to use results of pressuremeter tests in order to estimate the cohesion of these materials.

Carter *et al*. (1986) and Yu and Houlsby (1992) studied cavity expansion in cohesive-frictional materials, and developed expressions for cylindrical cavities which may be applied to interpretation of pressuremeter tests. These studies both assumed a linear elastic - perfectly plastic soil model, and an axi-symmetric, plane strain deformation scheme, and led to expressions relating both limit pressure, and the probe pressure versus radial displacement relation, to cohesion, c', friction angle, ϕ', dilation angle, ψ, elastic modulus, E, Poisson's ratio, ν, and in-situ effective lateral stress, p_0. Carter *et al.*'s solution was based on small-strain analysis, whereas Yu and Houlsby adopted large-strain analysis, more suitable for the plastic range of the pressuremeter tests. Consequently, Yu and Houlsby's solutions have been employed in the present work, considering kurkar to be a cohesive-frictional soil. The parameters c', ϕ' and ψ can, in principle, be obtained from Yu and Houlsby's expressions by trial and error, by assuming values and comparing the resulting, predicted pressure-displacement curves with those measured in field tests. In the particular case of kurkar, the triaxial value of ϕ' has been established to be 35°- 37°. For the plane-strain loading conditions relevant to pressuremeter testing, ϕ' would be expected to be about 1.1 times its triaxial value - i.e. about 41°. The dilation angle, ψ, may be estimated from ϕ', using published relations between the two. For example, Bolton (1986) suggested $\phi' = 0.8\psi + \phi'_{cv}$ where ϕ'_{cv} is the critical state friction angle, which for Israeli sands that form the skeleton of kurkar soils, is equal to 32° (Frydman 2000).

Consequently, ψ for the kurkar may be assumed to be about 11°. The Poisson ratio, ν, for kurkar may be assumed equal to about 0.25. The solutions of Yu and Houlsby (1992) may then be applied to estimate cohesion, c', from a pressuremeter test curve by adopting the above values of ϕ', ψ, and ν, and values of E and p_0 estimated from the field test curve (alternatively, p_0 may be estimated by other means). Various values of c' are assumed and for each a predicted probe pressure versus radial displacement (or probe volume change) curve is obtained and compared to the field curve.

Yu and Houlsby's solutions were used in order to estimate the cohesion from results of a pressuremeter test performed at a depth of 6 m in a kurkar profile in Tel-Aviv. The field test curve is shown, in its usual form of pressure versus cavity volume change, in Fig. 15, from which Ep = 48.3 MPa, and Er = 145.5 MPa. The limit pressure, p_L, was estimated by extrapolation (ASTM

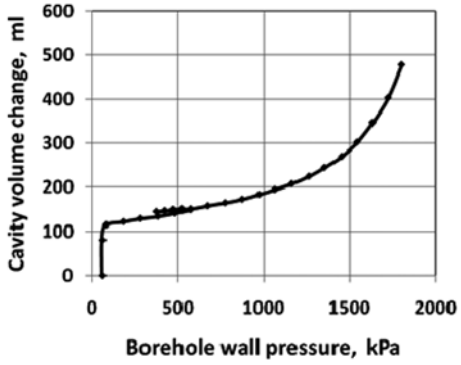

Fig. 15 Result of Menard pressuremeter test - Tel-Aviv, 6 m depth

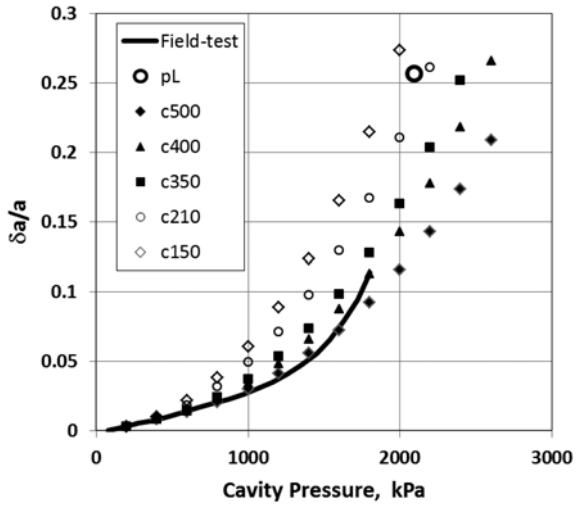

Fig. 16 Comparison between field tests and analytical solution according to Yu and Houlsby (1992)

2007), as the pressure which would expand the cavity to a volume of 2470 ml - twice its original value of 1235 ml (uninflated volume of probe + volume increase to bring it into firm contact with cavity wall), corresponding to a cavity wall displacement of 12 mm, or a radius of 46.73 mm. The limit pressure was so estimated to be 2.1 MPa. Fig. 16 shows a comparison of the field test result with theoretical curves obtained using Yu and Houlsby's solution. The latter curves used the values of ϕ', ψ and ν presented above, and a p_0 value of 80 kPa, corresponding to the point at which the slope of the field curve becomes linear. The elastic modulus was taken equal to Ep = 48.3 MPa. Different values of c' were assumed, and the resulting theoretical curves are shown for c' = 150kPa, 210 kPa, 350 kPa, 400 kPa and 500 kPa. The point corresponding to a limit pressure, p_L, of 2.1 MPa at a cavity radius of 46.73 mm is also shown. Good correspondence is seen in the linear (elastic) range between the field curve and the predicted curve corresponding to a cohesion, c' of 500 kPa. However, as the non-linear (plastic) deformations develop, the c' = 500 kPa curve is seen to depart from the field curve; the predicted curve shows more rigid behavior than the field curve. On the other hand, the predicted curves for c' = 150 kPa and 210 kPa depart from the field curve at a relatively small pressure, but correspond reasonably with the limit pressure. This observation is discussed further below.

4.3 Numerical analysis of pressuremeter test

As an alternative to use of existing, analytical cavity expansion solutions for estimation of c', as discussed above, numerical analyses (finite element or finite difference) of a pressuremeter test may be carried out, varying the geotechnical parameters until reasonable agreement is obtained with the field measurement. In the present study, use has been made of the code Flac (Itasca 2005), to simulate the Menard pressuremeter test performed in a kurkar profile in Tel-Aviv, at a depth of 6 m, presented above. The scheme analyzed is shown in Fig. 17. In order to limit the size of the overall mesh, the 6 m depth was modeled by taking the center of the pressuremeter probe at a depth of 2 m in a profile with a surface surcharge equivalent to 4 m of overburden. The analyses were performed

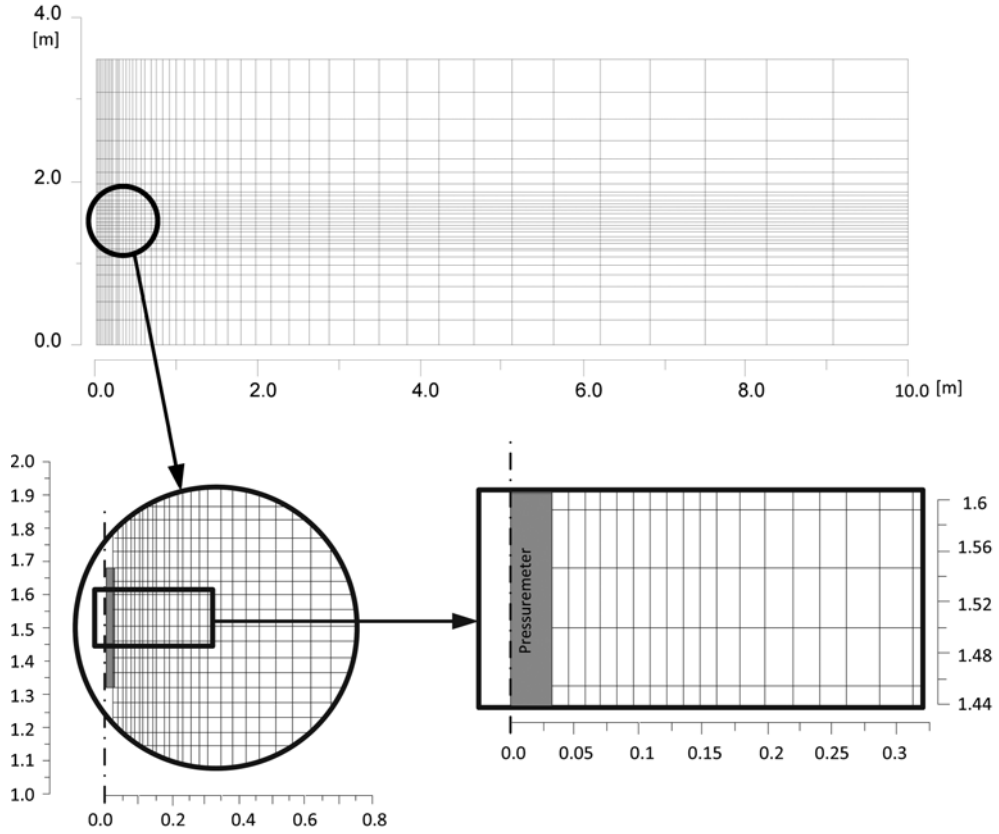

Fig. 17 Grid used for numerical analysis using Flac

by first establishing in-situ stresses in the profile (including the effect of the overburden pressure). For calculation of horizontal stresses, the coefficient of lateral earth pressure at rest was assumed equal to K_0 = 0.5-1.0; the analyses for K_0 = 0.5 yielded the best correspondence with the field test and these are presented here. The next stage of the analysis was intended to simulate the application of radial pressure by the pressuremeter subsequent to re-development of the in-situ lateral stress, p_0. Consequently, no excavation of the borehole was modeled, and the radial pressure was applied incrementally within the soil along the probe + guard-cell length, at its radius of 32 mm.

Several analyses were performed, with different assumed soil strength properties. Fig. 18 shows volume change versus applied pressure as obtained in the field test, and as calculated for (i) a linear-elastic soil, (ii) a linear-elastic - perfectly plastic soil with c' = 500 kPa, and (iii) a linear-elastic - perfectly plastic soil with c' = 200 kPa. For both values of c', results are shown for two assumptions with regards soil tensile strength, t, representing the upper and lower bounds to this value; (i) zero tensile strength, (ii) tensile strength corresponding to the extension of the linear Mohr-Coulomb strength envelope (i.e. $t = c'/tg\phi'$). This latter case would be consistent with the assumptions of the existing analytical solutions (Carter *et al*. 1986, Yu and Houlsby 1992). It is seen that the calculated curve for c' = 500 kPa and t = 570 kPa and the field curve extend along the linear-elastic curve, and depart from it at similar probe pressures. Thereafter, the calculated curve shows more rigid behavior, extending beyond the apparent field limit pressure of 2.1 MPa. This

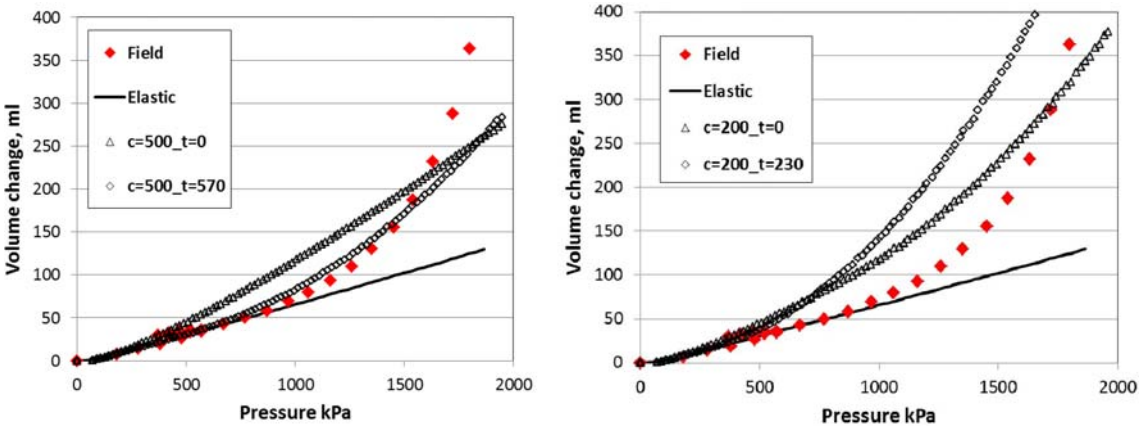

Fig. 18 Comparison between field test and numerical analyses

curve is basically similar to that based on the Yu-Houlsby analysis (Fig. 16). The importance of tensile strength is indicated from a comparison of the two curves calculated for $c' = 500$ kPa. The curve corresponding to zero tensile strength departs from the linear-elastic curve much earlier than do the field curve or the $t = 570$ kPa calculated curve. The curves calculated for $c' = 200$ kPa are seen to depart from the linear-elastic and the field test curves at a very low probe stress. The $t = 230$ kPa curve approaches the field curve towards the end of the field test.

The above observations are consistent with those made regarding the analytical solution of Yu and Houlsby (Fig. 16). The results tend to suggest that the kurkar has a cohesion of about 500 kPa in the early stage of loading, but that this decreases towards the end of the test. It would, therefore, appear that the kurkar soil strain-softens during loading. A number of analyses were carried out using Flac's strain-softening model, using different strength parameters and different extents of strain softening. Fig. 19 shows resulting curves found to approach the field test. Best correspondence was obtained for a material with cohesion, $c' = 500$ kPa and tensile strength, $t = 300$ kPa, both degrading to zero at a plastic shear strain of about 0.02. The correspondence for a material with c'

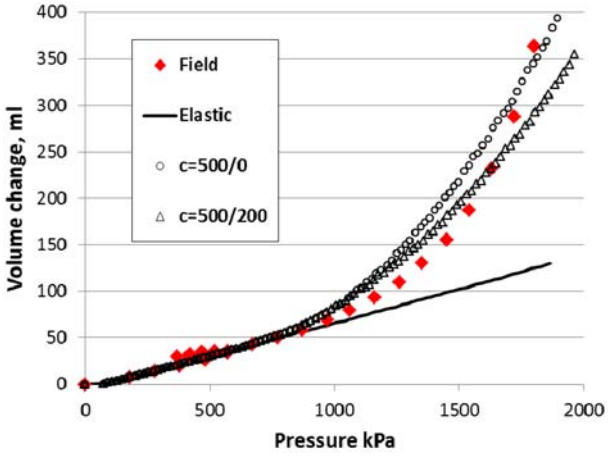

Fig. 19 Comparison between field test and numerical analyses, considering strain softening

degrading from 500 kPa to 200 kPa is seen to be less good. The apparent strain-softening behavior indicated by the numerical analyses is, in principle, consistent with the results of the triaxial tests shown in Figs. 6 and 7, although the maximum cohesion values found in those tests were considerably lower than the value estimated from the present field test. It would appear that the field pressuremeter test analyzed here was carried out in stronger material than that tested in the triaxial tests. However, the most significant conclusion in both cases is that the cohesion degenerated to close to zero with increasing strain. This indicates that although the kurkar soils may have significant cohesion in their undisturbed condition, this cohesion may be broken down during application of shear stresses, and caution must be displayed when considering the cohesion for design purposes.

5. Conclusions

The Menard pressure has been found to be a useful tool for characterizing the geotechnical properties of partially cemented sands, such as the kurkar soils found along the Israeli Mediterranean coast. The moduli of elasticity obtained from a pressuremeter test (*Ep* and *Er*) indicate strain-dependence of the soil rigidity. A relationship has been found between the rebound pressuremeter modulus (*Er*) and SPT blow count, which, while showing some scatter, is consistent with other published relations for granular soils, and with data presented by Burland and Burbidge (1985) relating footing settlements to SPT blow counts in granular soils. It appears that these relations are relevant to the kurkar soils since, despite their partial cementation, they behave, essentially, as granular materials. SPT blow counts or Er may be used for estimating footing settlements in these soils, but they must be modified to account for the *L/B* ratio of the footing.

By fitting the non-linear portion of the pressuremeter curve to predicted curves obtained from numerical analyses (finite element or finite difference), it is possible to obtain an estimate of the cohesion of the soil, for an assumed friction angle. The test reported in this paper indicated that the soil was strain-softening, and although it had a cohesion of the order of 500 kPa in the undisturbed condition and while loaded up to initial yield, this cohesion breaks down to effectively zero with increasing plastic shear strain. Consequently, it is recommended that caution be displayed when considering this initial cohesion for design purposes.

References

ASTM (2007), *Test method for prebored pressuremeter testing in soils*, ASTM Method D4719-07.

Baguelin, F., Jezequal, J.F. and Shields, D.H. (1978), *The pressuremeter and foundation engineering*, Trans. Tech. Publications, Clausthal, Germany.

Bakler, N., Denekamp, S. and Rohrlich, V. (1972), "Sandy units in the coastal plain of Israel: environmental interpretation using statistical analysis of grain size data", *Israel J. Earth Sci.*, **21**, 155-178.

Bolton, M.D. (1986), "The strength and dilatancy of sands", *Geotechnique*, **36**, 65-78.

Bowles, J.E. (1996), *Foundation analysis and design*, McGraw Hill, 5th edition.

Burland, J.B. and Burbidge, M.C. (1985), "Settlement of foundations on sand and gravel", *Proc. Institution of Civil Engineers, Part 1*, **78**, 1325-1381.

Carter, J.P., Booker, J.R. and Yeung, S.K. (1986), "Cavity expansion in cohesive frictional soils", *Geotechnique*, **36**(3), 349-358.

Clayton, C.R.I., Mathews, M.C. and Simons, N.E. (1995), *Site investigation*, Blackwell Science Ltd.
FHWA (2002), *Subsurface investigations - geotechnical site characterization*, Reference Manual, Publication FHWA NH1-01-031, U.S. Dept. of Transportation, Federal Highway Administration.
Frydman, S. (1979), "Use of the pressuremeter in clean and variably cemented sands", *Proc. 7th European Conf. on Soil Mech & Foundn Engng*., **2**. 217-222.
Frydman, S. (1982), *Calcareous sands of the Israeli coastal plain*, K.R. Demars and R.C. Chaney (ed), Geotechnical properties, behaviour and performance of calcareous soils, ASTM STP 777, 226-251.
Frydman, S. (1987), "Effect of confining pressure on Israeli calcalcareous sands", *Proc., 8th Asian Regional Conf. on Soil Mech. & Foundn Engng*., Kyoto, Japan, 167-171.
Frydman, S. (2000), "The shear strength of Israeli soils", *Israel J. Earth Sci*., **49**, 55-64.
Frydman, S., Melnik, J. and Baker, R. (1979), "The effect of prefreezing on the strength and deformation properties of granular soils", *Solids Found.*, **19**(4), 271-282.
Frydman, S., Hendron, D., Horn, H., Steinbach, J., Baker, R. and Shaal, B. (1980), "Liquefaction study of cemented sand", *J. Geotech. Eng. Div. - ASCE*, **106**(GT3), 275-297.
Gavish, E. and Friedman, G.M. (1969), "Progressive diagenesis in quaternary to late tertiary sediments: sequence and timescale", *J. Sediment. Petrology*, **39**, 980-1006.
Gibson, R.E. and Anderson, W.F. (1961), "In-situ measurement of soil properties with the pressuremeter", *Civil Eng. Public Works Rev.*, **56**(658), 615-618.
Giraud, J.P. (1968), "Settlement of a linearly loaded rectangular area", *J. Soil Mech. Found. Div. - ASCE*, **94**(SM4), 813-831.
Hughes, J.M.O., Wroth, C.P. and Windle, D. (1977), "Pressuremeter tests in sand", *Geotechnique*, **22**, 451-457.
Komornik, A., Wiseman, G. and Frydman, S. (1969), "A study of in situ testing with the pressuremeter", *Proc. Conf. on In situ Investigations in Soils and Rocks*, Inst. of Civil Eng., London, 145-154.
Lunne, T. and Christoffersen, H.C. (1985), "Interpretation of cone penetrometer data for offshore sands", *Norw. Geotech. Tech. Pub.*, **156**, 1-12.
Mair, R.J. and Muir Wood, D. (1987), *Pressuremeter testing: methods and interpretation*, Butterworths, Boston.
Menard, L. (1975), "The interpretation of pressuremeter test results", *Sols Soils*, **26**, 7-43.
Palmer, A.C. (1972), "Plane strain expansion of a cylindrical cavity in clay: a simple interpretation of the pressuremeter test", *Geotechnique*, **22**, 451-457.
Schmertmann, J.H. (1970), "Static cone to compute static settlement over sand", *J. Soil Mech. Found. Div. - ASCE*, **96**(13), 1011-1043.
Stroud, M.A. (1988), "The standard penetration test - its application and interpretation", *Proc., Penetration Testing in the U.K*., I.C.E., Thomas Telford, London, 29-48.
Taylor, D.W. (1937), "Stability of earth slopes", *J. Boston Soc. Civil Eng.*, **24**(3), Reprinted in: *Contributions to Soil Mechanics 1925 to1940*, Boston Society of Civil Engineers, 337-386.
Weiher, B. and Davis, R. (2004), "Correlation of elastic constants with penetration resistance in sandy soils", *Int. J. Geomech.*, **4**(4), 319-329.
Wiseman, G., Hayati, G. and Frydman, S. (1981), "Stability of heterogeneous sandy coastal cliff", *Proc., 10th International Conf. on Soil Mech. & Foundn Engng*, 569-574.
Yu, H.S. and Houlsby, G.T. (1991), "Finite cavity expansion in dilatant soils: loading analysis", *Geotechnique*, **41**(2), 173-183.

GM